Genetic Reconstruction of Mouse Spermatogonial Stem Cell Self-Renewal In Vitro by Ras-Cyclin D2 Activation

Jiyoung Lee,[1,5] Mito Kanatsu-Shinohara,[1] Hiroko Morimoto,[1] Yasuhiro Kazuki,[2] Seiji Takashima,[1] Mitsuo Oshimura,[2] Shinya Toyokuni,[3] and Takashi Shinohara[1,4,*]

[1]Department of Molecular Genetics, Graduate School of Medicine, Kyoto University, Kyoto 606-8501, Japan
[2]Department of Molecular and Cell Genetics, School of Life Sciences, Faculty of Medicine, Tottori University, Yonago, Tottori 683-8503, Japan
[3]Department of Pathology and Biological Responses, Graduate School of Medicine, Nagoya University, Nagoya 466-8550, Japan
[4]Japan Science and Technology Agency, CREST, Kyoto 606-8501, Japan
[5]Present address: Global Center of Excellence Program, Tokyo Medical and Dental University, Tokyo 113-8510, Japan
*Correspondence: tshinoha@virus.kyoto-u.ac.jp
DOI 10.1016/j.stem.2009.04.020

SUMMARY

Spermatogonial stem cells (SSCs) undergo self-renewal division and support spermatogenesis. Although several cytokines coordinate to drive SSC self-renewal, little is known about the mechanisms underlying this process. We investigated the molecular mechanism by reconstructing SSC self-renewal in vitro without exogenous cytokines. Activation of Ras or overexpression of cyclins D2 and E1, both of which were induced by Ras, enabled long-term self-renewal of cultured spermatogonia. SSCs with activated Ras responded properly to differentiation signals and underwent spermatogenesis, whereas differentiation was abrogated in *cyclin* transfectants after spermatogonial transplantation. Both *Ras*- and *cyclin*-transfected cells produced seminomatous tumors, suggesting that excessive self-renewing stimulus induces oncogenic transformation. In contrast, cells that overexpressed cyclin D1 or D3 failed to make germ cell colonies after transplantation, which indicated that cyclin expression pattern is an important determinant to long-term SSC recolonization. Thus, the Ras-cyclin D2 pathway regulates the balance between tissue maintenance and tumorigenesis in the SSC population.

INTRODUCTION

Spermatogenesis is a complex process that originates from a small population of spermatogonial stem cells (SSCs). A single SSC can produce two stem cells (self-renewing division) or two differentiated cells (differentiating division) (Meistrich and van Beek, 1993; de Rooij and Russell, 2000). However, analysis of SSC self-renewal has been hampered by the lack of functional assays for SSCs and the lack of a culture system to recapitulate SSC self-renewal. The first problem made it impossible to study self-renewal, because SSCs can be determined only retrospec-

tively by analyzing daughter cell types produced by mitosis. Although SSCs can be identified by whole mounts of seminiferous tubules in vivo, distinguishing SSCs from progenitors by morphology or marker expression is impossible in vitro. This problem was resolved by the development of a germ cell transplantation technique (Brinster and Zimmermann, 1994). The microinjection of dissociated testis cells into empty seminiferous tubules of infertile male mice resulted in long-term reconstitution of the host testis and the production of germ cell colonies.

The lack of a culture system to recapitulate SSC self-renewal in vitro was another major hurdle. The first clue to the mechanism of SSC self-renewal came from gene-targeting studies. Glial cell line-derived neurotrophic factor (GDNF) belongs to the transforming growth factor-β superfamily and is expressed in Sertoli cells, which support spermatogenesis. Heterozygous knockout mice for GDNF gradually lost spermatogenesis due to SSC depletion, whereas overexpression of GDNF produced clusters of undifferentiated spermatogonia that could not differentiate (Meng et al., 2000). In 2003, we established a method to induce SSC self-renewal in vitro. The cultured cells, which we designated germline stem cells (GSCs), expressed spermatogonia markers and were able to differentiate into sperm when they were transplanted into seminiferous tubules. Unlike embryonic stem cells (ESCs), GSCs are stable in their karyotype and DNA methylation patterns and are amenable for gene targeting (Kanatsu-Shinohara et al., 2003, 2006). The development of a SSC culture system provided an opportunity to collect large numbers of SSCs for biochemical and molecular analyses.

Although a series of molecular events triggered by GDNF have been well characterized in somatic cell types, much of the molecular machinery for SSC self-renewal remains unknown. Studies are complicated because SSC self-renewal depends on several cytokines. GSCs proliferate when GDNF is supplemented with basic fibroblast growth factor (bFGF) or epidermal growth factor (EGF) (Oatley and Brinster, 2008). In our previous work, we found that inhibition of the phosphoinositide-3 kinase (PI3K)-Akt pathway, a signaling pathway downstream from GDNF or FGF receptors, abrogates SSC self-renewal (Lee et al., 2007). However, activation of Akt alone was not sufficient to drive SSC self-renewal but also required costimulation of bFGF, and not EGF. Despite the increasing number of identified
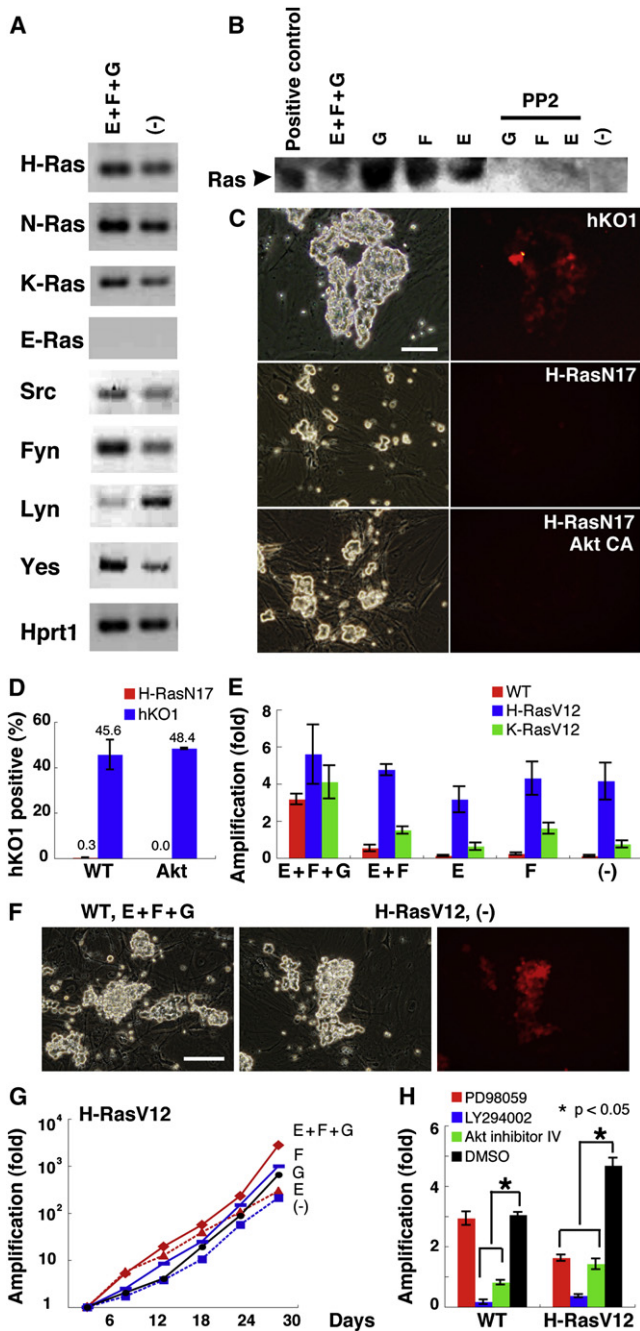
Figure 1. Expression and Function of *Ras* in GSCs

(A) RT-PCR analysis of GSCs. GSCs on laminin were cultured under the indicated conditions for 6 days, and samples were collected for RT-PCR analysis.

(B) Activation of Ras by exogenous cytokines. GSCs on laminin were starved for 4 days, and then the indicated cytokines were added to the culture medium. Where indicated, cells were also incubated 2 hr before cytokine treatment with PP2. The samples were collected after 15 min. Addition of PP2 inhibited activation in all cases.

(C) Appearance of GSC colonies on MEFs after *H-RasN17* transfection. A lentivirus vector expressing both H-RasN17 and hKO1 was transduced into WT (top, middle) and Akt-GSCs (bottom). While GSCs transduced with control empty vector survived after 12 days, few cells survived after *H-RasN17* transfection.

(D) Effect of H-RasN17 on WT and Akt-GSC growth on MEFs. The number of colonies showing hKO1 fluorescence was counted 12 days after transfection

genes involved in SSC self-renewal (Oatley and Brinster, 2008), how the exogenous cytokine signals are converted to drive SSC self-renewal machinery has remained unclear.

In general, stem cells in self-renewing tissues divide only infrequently, and self-renewing signals may control cell division by acting on the G1 phase of the cell cycle. Mammals possess three types of cyclin D (cyclin D1–D3), and regulation of their expression is critical in the progression of the cell cycle (Sherr and Roberts, 2004). Moreover, the three subtypes are expressed in distinct patterns in undifferentiated spermatogonia. In the adult testis, cyclins D1 and D3 are expressed in spermatogonia at all cycle stages of the seminiferous tubule epithelium (Beumer et al., 2000). However, cyclin D2 is expressed in the nuclei of spermatogonia present around stage VIII of the cycle, when A_{al} spermatogonia differentiate into A_1 spermatogonia, suggesting that cyclin D2 is involved in differentiation. The specific expression patterns of cyclins suggest that they have unique and important roles in determining the types of SSC division.

Here, we analyzed SSC self-renewal mechanisms by reconstructing SSC self-renewal in vitro without self-renewal factors. Applying germ cell transplantation and GSC culture techniques, we found that Ras and a specific subtype of cyclin induce self-renewal without exogenous cytokines and tumorigenesis of SSCs.

RESULTS

Activated Ras Induces GSC Self-Renewal In Vitro

To clarify the signaling pathway of SSC self-renewal, we analyzed the involvement of *Ras* proto-oncogene, because GDNF and EGF/bFGF activate Ras in somatic cells (Takahashi, 2001; Danielsen and Maihele, 2002; Thisse and Thisse, 2005). Reverse transcriptase-polymerase chain reaction (RT-PCR) analysis showed that GSCs express all three classic isoforms of Ras (H-Ras, N-Ras, and K-Ras), but we could not detect ES cell-specific E-Ras (Figure 1A). To test whether Ras is activated under GSC culture conditions, we performed a pull-down assay using a GST-fusion protein containing the Ras-binding domain of Raf1 to precipitate active Ras. Immunoblotting using anti-Ras antibody revealed that Ras was activated by adding EGF, bFGF, or GDNF (Figure 1B). This activation was inhibited by an Src inhibitor (PP2), which was previously shown to be involved

(n = 3). A cluster of cells was defined as a colony when it contained more than five cells.

(E) Effect of cytokines on H-RasV12-GSC and K-RasV12-GSC growth after 6 days of culture on MEFs (n = 5). While H-RasV12-GSCs grew without cytokines, K-RasV12-GSCs did not proliferate without bFGF.

(F) Appearance of WT cells (left) and H-RasV12-GSC (middle and right) on MEFs. H-RasV12-GSCs retained normal morphology under cytokine-free conditions. The efficient transduction is evidenced by red fluorescence (right).

(G) Growth curve for H-RasV12-GSCs maintained on MEFs. H-RasV12-GSCs grew exponentially under all conditions.

(H) Effect of the PI3K-Akt pathway on GSC growth on MEFs for 6 days. WT GSCs were cultured with cytokines, but H-RasV12-GSCs were cultured without cytokines (n = 6). Whereas only LY294002 and Akt inhibitor IV inhibited growth of WT GSCs, all inhibitors had a significant negative effect on H-RasV12-GSCs.

Scale bar, 100 μm (C and F). E, EGF; F, bFGF; G, GDNF. Error bars indicate SEM.

in SSC and spermatogonia proliferation (Braydish-Stolle et al., 2007; Oatley and Brinster, 2008). RT-PCR analyses also confirmed the presence of at least four types of Src family molecules in GSCs (Figure 1A).

To directly examine whether Ras is necessary for GSC proliferation, we conducted two sets of experiments using H-RasN17, a dominant-negative Ras isoform that inhibits the three Ras isoforms. In the first set of experiments, wild-type (WT) GSCs were infected with *CSII-EF-H-RasN17-IRES2-hKO1* lentivirus, which expresses H-RasN17 as well as humanized Kusabira-Orange 1 (hKO1) fluorescent marker gene. Three days after infection, GSCs stopped proliferating, and almost all cells died by day 12 (Figure 1C). In contrast, cells transfected with an empty vector proliferated normally and expressed the hKO1 marker. The number of colonies in *H-RasN17* transfectant was 0.7% of that in control vector transfectants 12 days postinfection (Figure 1D). In the second set of experiments, we used the same lentivirus vector to transduce GSCs that expressed constitutively active Akt (Akt-GSCs). We previously showed that the expression of activated Akt could replace GDNF to induce the proliferation of GSCs in the presence of bFGF (Lee et al., 2007). Introducing *H-RasN17* abrogated the growth of Akt-GSCs, and the cells died within 12 days, with similar kinetics as WT GSCs (Figure 1D). Together, these experiments showed that Ras is necessary for GSC proliferation and/or survival.

Then we examined whether Ras is sufficient for GSC proliferation. It is known that the activities of the three Ras isoforms are slightly different: N- and K-Ras are more potent than H-Ras in mitogen-activated protein kinase activation, while H-Ras is more potent than N- and K-Ras in PI3K activation (Yan et al., 1998; Li et al., 2004). To examine which of the two pathways plays a predominant role in SSC self-renewal, we produced two types of transfectants using activated forms of H-Ras (H-RasV12) and K-Ras (K-RasV12). In agreement with previous observations, the two Ras isoforms exhibited different biological activities in GSCs. Overall, *H-RasV12*-transfected GSCs (H-RasV12-GSCs) grew significantly better than *K-Ras*-transfected cells (K-RasV12-GSCs) (Figure 1E). Moreover, whereas K-RasV12-GSCs depended on bFGF for continuous proliferation, H-RasV12-GSCs proliferated without cytokines (Figure 1E).

Because these results suggested that H-Ras drives SSC self-renewal more efficiently, we focused on H-RasV12-GSCs in subsequent experiments. Although the morphology of the colony did not change after transfection (Figure 1F), H-RasV12-GSCs grew by ≥5-fold during a 6-day culture, while WT GSCs proliferated up to ~3-fold, suggesting that H-RasV12 sensitized GSCs to exogenous cytokine stimuli (Figure 1E and 1G). The growth of both WT and H-RasV12-GSCs depended on the PI3K-Akt pathway because both LY294002 (a PI3K-specific inhibitor) and Akt inhibitor IV stopped their proliferation (Figure 1H). Moreover, PD98059, a MEK-specific inhibitor, interfered with H-RasV12-GSC growth, suggesting that the MEK pathway helps facilitate H-RasV12-GSC proliferation.

To clarify the mechanism of enhanced cell cycling, we analyzed potential downstream genes involved in cell cycling. Real-time PCR analyses showed that H-RasV12-GSCs upregulated immediate-early gene c-*Myc* as well as the cyclin D/cdk4 inhibitor *p16*, but no significant upregulation of a major cyclin
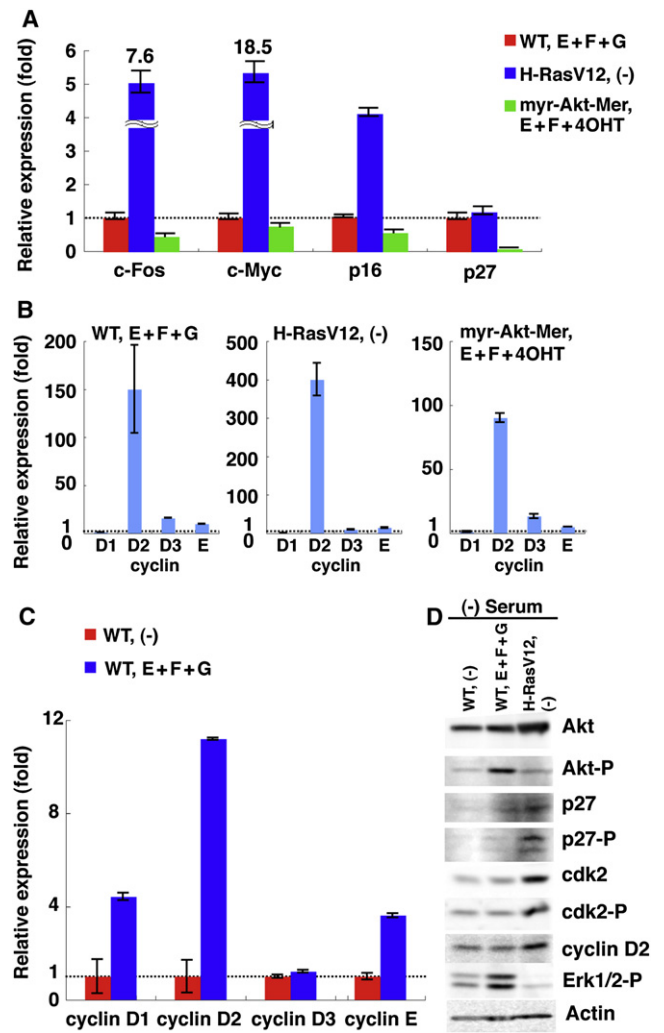

Figure 2. Analysis of Downstream Signaling of H-RasV12 in GSCs
(A) Real-time PCR analysis of H-RasV12-GSCs (n = 3). Cells were cultured on laminin for 6 days under the indicated conditions. The values were normalized to *Hprt1* expression, with expression levels in WT GSCs cultured with cytokines.
(B) The patterns of *cyclin* expression during culture on laminin. The values were normalized to *Hprt1* expression, with expression levels of *cyclin D1*.
(C) Induction of *cyclin* expression in WT GSCs on laminin. Cells were stimulated with the indicated cytokines for 24 hr. The values were normalized to *Hprt1* expression, with expression levels in cells cultured without cytokines.
(D) Western blot analysis of WT and H-RasV12-GSCs. The cells were starved on laminin for 4 days, and then WT GSCs were either treated or not treated with the indicated cytokines. Treated cells were recovered 30 min after treatment. E, EGF; F, bFGF; G, GDNF. Error bars indicate SEM.

E/cdk2 inhibitor *p27* was found (Figure 2A). Both WT and H-RasV12-GSCs showed strong expression of *cyclin D2* (Figure 2B). The strong induction of *cyclin D* in WT GSCs was evident by 24 hr after cytokine stimulation. Whereas *cyclin D2* was upregulated most dramatically, *cyclin D3* did not change significantly (Figure 2C). These patterns of *cyclin* expression were generally similar in GSCs expressing myristoylated-Akt-Mer protein (Akt-Mer-GSCs), which proliferate when cultured with 4-hydroxytamoxyfen (4OHT) and bFGF (Lee et al., 2007).
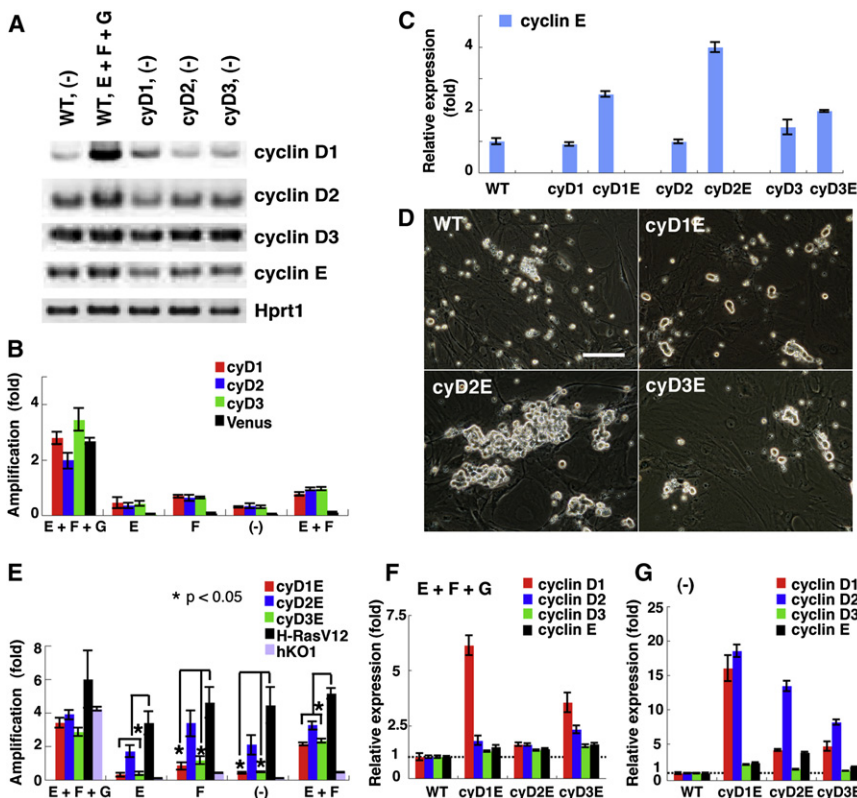
Figure 3. GSC Proliferation by Cyclin Transfection

(A) RT-PCR analysis of *cyclin* expression in *cyclin D*-transfected cells. The cells were cultured on laminin for 24 hr under the indicated conditions.

(B) Effect of cytokines on *cyclin*-transfected GSC growth. WT GSCs were transfected with *cyclin D* genes. The cells were cultured under the indicated conditions on MEFs for 6 days.

(C) Increased expression of *cyclin E* after additional *cyclin E* transfection (n = 6). The cells were cultured on laminin for 24 hr without cytokines. Values were normalized to *Hprt1* expression, with expression levels in WT GSCs.

(D) Appearance of *cyclin*-transfected cells cultured without cytokines on MEFs for 6 days. Only cyD2E-GSCs formed germ cell colonies.

(E) Effect of cytokines on GSCs that were transfected with *cyclin D* and *E*. While H-RasV12-GSCs and cyD2E-GSCs grew without cytokines, cycD1E-GSCs and cyD3E-GSCs grew when they were supplemented with EGF and bFGF. The cells were cultured on MEFs for 6 days.

(F and G) Real-time PCR analysis of *cyclin*-transfected GSCs (n = 6). Cells were cultured with (F) or without (G) cytokines on laminin for 24 hr. Values were normalized to *Hprt1* expression, with expression levels in WT GSCs.

Scale bar, 100 μm (D). E, EGF; F, bFGF; G, GDNF. Error bars indicate SEM.

However, the level of *p27* expression was significantly lower in these cells than in other cell types (Figure 2A).

Western blot analysis confirmed the greater expression of cyclin D2 in H-RasV12-GSCs (Figure 2D). Although Akt and both Erk1 and 2 were rapidly phosphorylated after cytokine stimulation in WT GSCs, phosphorylation of Erk1 did not occur in H-RasV12-GSCs, and the levels of phosphorylation of Akt and Erk2 did not change significantly compared with WT GSCs without cytokines. However, H-RasV12-GSC exhibited increased production and phosphorylation of p27 at Thr 187. Because Thr 187 phosphorylation is mediated by the cyclin E-cdk2 complex and is required for ubiquitin-mediated degradation (Slingerland and Pagano, 2000), these results suggest that an increased amount of p27 is produced but rapidly destructed in H-RasV12-GSCs. The increase in phosphorylation of cdk2 at Thr 160 suggests a high level of cdk-activating kinase activity in H-RasV12-GSCs. Because newly synthesized cyclin D associates with p27 and overexpression of cyclin D2 induces translocation of p27 from the nucleus (Susaki et al., 2007), these results strengthen the hypothesis that Ras activation facilitates the G1/S transition by rapid and strong induction of cyclin D2 expression and promotion of p27 export from the nucleus.

Enhanced GSC Proliferation by Overexpression of Cyclin Genes

To test this hypothesis, we introduced *cyclin D1*, *D2*, and *D3* genes into WT GSCs by lentivirus vectors that coexpressed Venus under the *Eif1a* promoter. Almost all GSCs were successfully infected by each vector. However, GSCs engineered to constitutively express each *cyclin D* gene depended on exogenous cytokines, and the levels of *cyclin* expression did not change significantly (Figures 3A and 3B). Cotransfection of two different or all three *cyclin D* genes did not improve the GSC growth (data not shown).

Because cyclin E plays a major role in the G1/S transition and was strongly upregulated in WT GSCs, we postulated that transfection of *cyclin E* might trigger efficient growth. Although cyclin E1 alone did not induce GSC proliferation, cotransfection of *cyclin D* and *E1* restored GSC growth (Figures 3C–3E and Figure S1 available online), indicating a synergistic effect of cyclin D and E in driving the cell cycle. For example, *cyclin D2 + E1* double transfectants (cyD2E-GSCs) expanded 2-fold without cytokines. Moreover, cells that expressed cyclin D1 + E1 (cyD1E-GSCs) or cyclin D3 + E1 (cyD3E-GSCs) grew when they were cultured only with EGF and bFGF (Figure 3E), suggesting that cyclins D1 or D3 may partly compensate for GDNF. The levels of *cyclins* changed dramatically by exogenous cytokines (Figures 3F and 3G). While real-time PCR confirmed the upregulation of *cyclins D1* and *D2* when the cells were cultured without cytokines, increase was evident only in *cyclin D1* when the cells were cultured with cytokines. This is probably because expression of *cyclin D1* is relatively weaker than that of *Eif1a* (Figure S2). Only modest increase of *cyclin D3* was found after *cyclin D3* transfection regardless of culture conditions. The cells, however, showed upregulation of *cyclins D1* and *D2*. Similar ectopic upregulation of *cyclin D2* was also noted in cyD1E-GSCs. Taken together, these results demonstrate that a combination of cyclins D2 and E can mimic H-RasV12 and induces GSC proliferation without self-renewal factors.
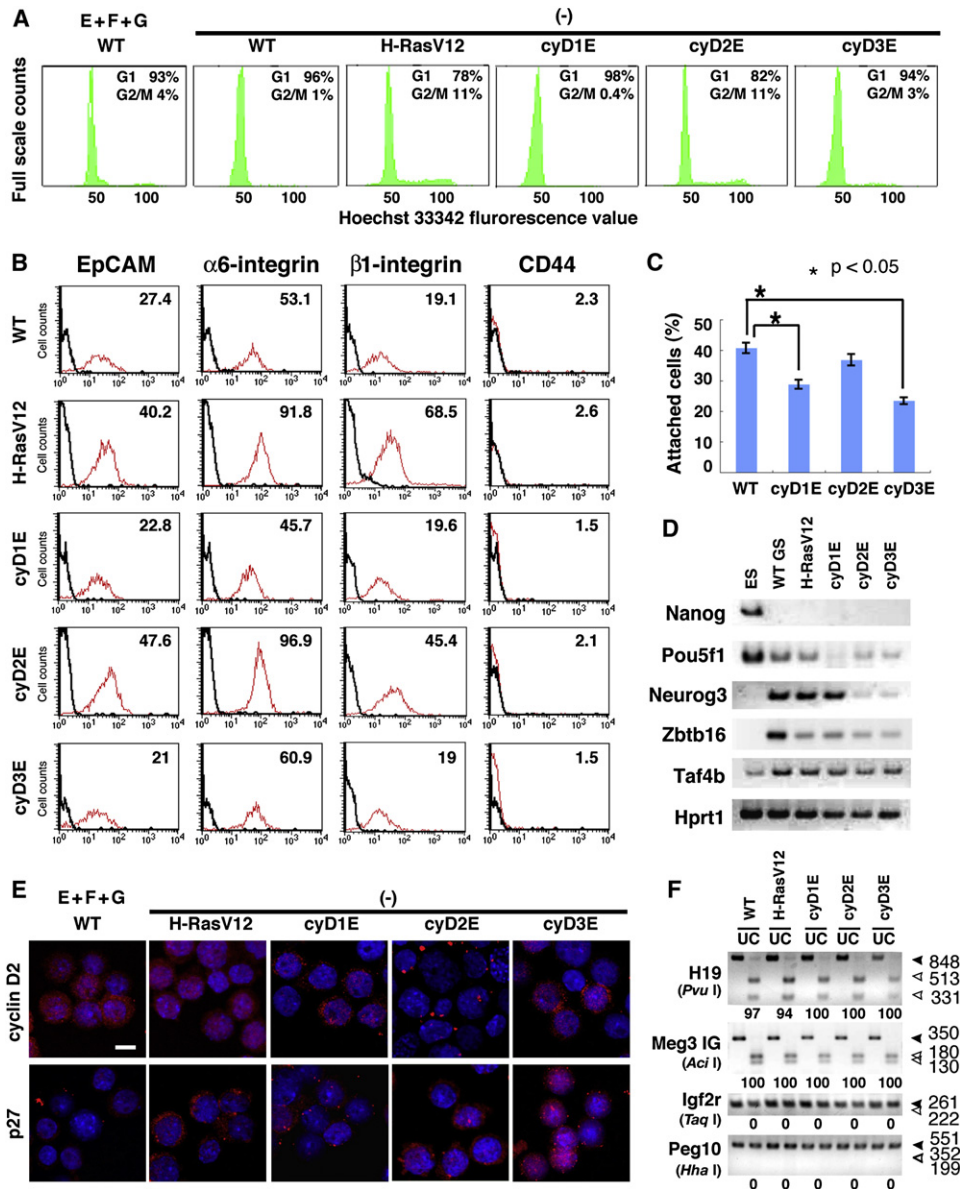
Figure 4. Phenotypic Characterization of H-RasV12-GSCs and *cyclin*-Transfected Cells

(A) Cell-cycle distribution. Significantly more cells are in the G2/M phase in the H-RasV12-GSCs and cyD2E-GSCs.

(B) Characterization of cell surface antigens by flow cytometry. Note the weaker expression of EpCAM and α6- and β1-integrin in cyD1E-GSCs and cyD3E-GSCs. Red line, specific antibody; black line, unstained control. Values indicate mean fluorescence intensity.

(C) Statistically significant reduction in laminin binding of cyD1E- and cyD3E-GSCs.

(D) RT-PCR analysis. *Neurog3* expression was weaker in both cyD2E- and cyD3E-GSCs.

(E) Immunocytochemistry of p27 and cyclin D2 in transfected cells. The transfectants were cultured on laminin without cytokines for 6 days and stained with anti-cyclin D2 (top) or p27 (bottom) antibody. Cyclin D2 was strongly expressed in both WT and H-RasV12-GSCs. p27 staining was predominantly found in the cytoplasm of H-RasV12-GSCs and cyD2E-GSCs, whereas nuclear staining was found in cyD1E-GSCs and D3E-GSCs. Counterstained by DAPI.

(F) COBRA. Open arrows indicate the sizes of the methylated DNA, whereas closed arrows indicate the size of the unmethylated DNA. Percent methylation, as estimated by the intensity of each band, is indicated below the gels. U, uncleaved; C, cleaved.

Scale bar, 10 μm (E). E, EGF; F, bFGF; G, GDNF. Error bars indicate SEM.

Phenotypic Analyses of Cultured Cells

Next we compared the phenotype of the all types of transfectants. In good agreement with cell recovery, cell-cycle analyses showed more cells in the G2/M phase in H-RasV12-GSCs and cyD2E-GSCs than in WT GSCs cultured without cytokines, but significantly more cyD1E-GSCs and cyD3E-GSCs were in the G1 phase (Figure 4A). Flow cytometry also showed that the transfected cells expressed SSC markers, including EpCAM and α6- and β1-integrin (Figure 4B). SSEA-1, a marker of ES cells, was not expressed in the transfectants, and the levels of

c-kit expression did not change significantly (data not shown), suggesting that the transgenes did not alter the proportion of SSCs. However, both H-RasV12-GSCs and cyD2E-GSCs showed increased expression of EpCAM and α6- and β1-integrin compared to WT GSCs. When *cyclin*-transfected cells were added to laminin-coated plates, binding was most significantly impaired in cyD3E-GSCs (Figure 4C).

In addition to the cell surface phenotype, RT-PCR revealed weaker expression of *Pou5f1* and *Zbtb16* in *cyclin*-transfected cells (Figure 4D). *Neurog3*, a marker of differentiating SSCs, was expressed strongly in WT, H-RasV12-, and cyD1E-GSCs, but it was weaker in both cyD2E- and cyD3E-GSCs. On the other hand, *Taf4b* was expressed at the same levels in different kinds of GSCs, and no *Nanog* expression was found. Immunocytochemical analysis further showed that *cyclin* transfection influenced the distribution of p27 (Figure 4E). While p27 is present predominantly in the cytoplasm of both H-RasV12-GSCs and cyD2E-GSCs, a strong p27 signal was found in the nucleus of cyD3E-GSCs. The cyD1E-GSCs exhibited weaker but distinct punctate staining in the nucleus. When the cells were stained with anti-cyclin D2 antibody, both WT and H-RasV12-GSCs showed strong expression in both the cytoplasm and nucleus, whereas only weaker signals were found in cyD1E-GSCs and cyD3E-GSCs. Notably, cyD2E-GSCs showed only punctate cyclin D2 staining, suggesting that other molecules might have influenced their localization.

Despite the differences in growth characteristics, combined bisulfite restriction analysis (COBRA) showed that DNA methylation of differentially methylated regions (DMRs) in two paternally imprinted genes (*H19* and *Meg3* IG) and two maternally imprinted genes (*Igf2r* and *Peg10*) were of typical androgenetic DNA methylation patterns, including hypermethylation of *H19* and *Meg3* IG DMRs and hypomethylation of *Igf2r* and *Peg10* DMRs (Figure 4F). Taken together, these results show that the cultured cells had normal spermatogonia phenotypes but also suggest that they had different functions.

Examination of SSC Activity by Germ Cell Transplantation

Finally, we used the germ cell transplantation technique to confirm the effects of transgenes. Cells cultured on mouse embryonic fibroblasts (MEFs) without cytokines were transplanted into the seminiferous tubules of congenitally infertile WBB6F1-W/W^v (W) mice. Because spermatogenesis in W mice is arrested in undifferentiated type A spermatogonia, they serve as recipients for donor SSC colonization (Brinster and Zimmermann, 1994). In the first set of experiments, all four types of transfected cells (4×10^6 cells for each testis) were transplanted into W mice. At the time of transplantation, all cells expressed fluorescence under UV light, indicating that they contained the transgenes. When recipient testes were analyzed after 3 months, only H-RasV12-GSCs and cyD2E-GSCs produced germ cell colonies (Figure 5A). In contrast, no fluorescence was observed in testes that received cyD1E-GSCs. We occasionally found scattered green germ cells in the testes of cyD3E-GSC recipients (Figure 5A, inset), suggesting that cyclin D3 overexpression had an impact on SSCs. However, these cells did not grow into distinct colonies. The recipient testes with germ cell colonies were significantly larger than those

without colonies, reflecting the greater degree of donor-derived colonization (Figure 5B).

In the second set of experiments, we transplanted H-RasV12-GSCs and cyD2E-GSCs at different time points in culture to quantify the increase in SSC numbers. A sample of cells was recovered for transplantation at three different time points during consecutive passages. SSC numbers increased in cultures of both transfectants. Approximately 5.5×10^5-fold expansion of SSCs was observed during 76 days of H-RasV12-GSC culture, whereas SSCs in cyD2E-GSC culture grew by 2.2×10^6-fold in 78 days (Table 1). Assuming that 10% of the transplanted cells colonized each recipient testis (Nagano et al., 1999), the concentration of SSCs in culture ranged from 0.1% to 2.7%, which is within the range of previous results with WT GSCs (Oatley and Brinster, 2008).

Tumor Development from H-RasV12-GSCs and cyD2E-GSCs

Although both H-RasV12-GSCs and cyD2E-GSCs formed germ cell colonies, some were irregularly shaped, suggesting abnormal differentiation (Figure 5C). However, both types of cells maintained normal karyotype before transplantation, suggesting that abnormal spermatogenesis was not caused by defective karyotype (Figure 5D). Thus we analyzed differentiated germ cells by RT-PCR, which revealed the expression of normal differentiation markers in recipients of WT and H-RasV12-GSCs (Figure 5E). Recipient testes expressed genes not only in zygotene- to diplotene-spermatocyte stages, such as *Sycp1* and *Sycp3*, but also in the pachytene spermatocyte stage and later, including *Clgn*, *Hoxa4*, *Piwil1*, and *Crem*. In contrast, differentiation was significantly limited in testes that received cyD2E-GSCs. Histological analyses indicated normal spermatogenesis in five of six H-RasV12-GSC recipient testes (Figure 5F). In total, 38.3% ± 8.1% (167/377 tubules in the six testes) of the tubules contained spermatogenesis. However, seminomatous tumors occurred in all testes that received H-RasV12-GSCs (Figure 5F). The tumors were composed of round cells with little cytoplasm and invaded testicular interstitial tissues in all cases.

Germ cell tumors (GCTs) were also found in all five recipient testes with cyD2E-GSCs. However, they were distinct from the H-RasV12-induced tumors in that they were not accompanied by normal spermatogenesis. Although 39.2% ± 5.9% (216/548 tubules in the five testes) of the tubules contained multiple layers of germ cells, they consisted of clusters of spermatogonia and no haploid cells. Moreover, unlike the H-RasV12-induced tumors, no signs of local tumor invasion were observed, suggesting a distinct characteristic of tumor. No distant metastasis or lymphocyte infiltration was seen in either tumor type. Immunohistological analyses showed that both types of tumors expressed placental alkaline phosphatase (PLAP; Figure 5G), which is normally downregulated in the postnatal testis and is a marker of seminomas (Meng et al., 2001). Flow cytometry revealed weak expression of CD44, a cancer stem cell antigen (Visvader and Lindeman, 2008), in both types of cell recipients (Figure 5H). CD44 expression was not detected in the WT GSC recipients. Subcutaneous injection of H-RasV12- and cyD2E-GSCs did not produce tumors.

To examine whether the GCTs contain cancer stem cells, we performed serial transplantation. Single cell suspensions from
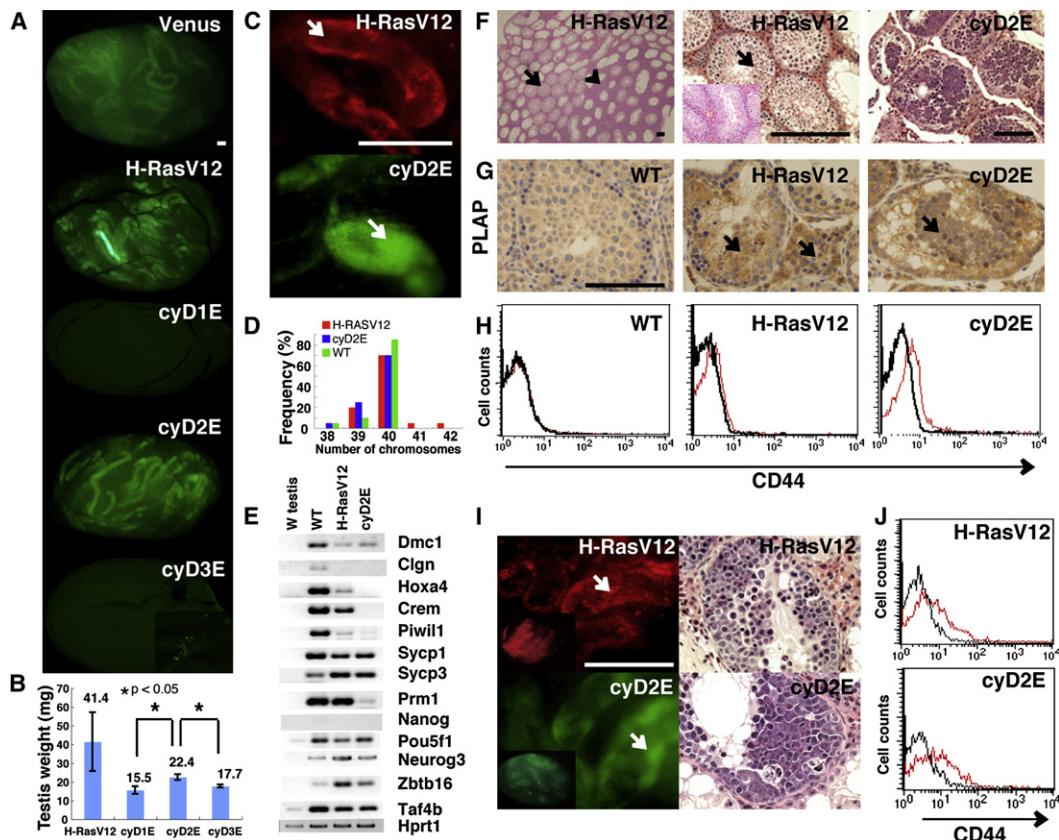
Figure 5. SSC Activity of Cultured Cells

(A) Appearance of recipient testes. Only H-RasV12-GSCs and cyD2E-GSCs produced germ cell colonies. Clusters of germ cells were occasionally observed in the recipient testis with cyD3E-GSCs (inset).

(B) Testis weights after transplantation.

(C) Abnormal germ cell clumps found in the testes of H-RasV12- and cyD2E-GSC recipients (arrows).

(D) Normal karyotype of the cultured cells. At least 20 cells were counted.

(E) RT-PCR analyses of recipient testes. The expression of haploid markers was reduced in cyD2E-GSC recipients.

(F) Histology of recipient testes. Spermatogenesis was observed only in H-RasV12-GSC recipients (arrows). Abnormal spermatogonia proliferation was detected in both H-RasV12-GSCs and cyD2E-GSCs. Interstitial tumor infiltration was found in H-RasV12-GSC recipients (arrowhead). Normal spermatogenesis was found in the control transplant with an empty vector (inset).

(G) Immunohistochemistry of recipient testes. GCT was positive for PLAP (arrows). Counterstained by hematoxylin.

(H) CD44 expression in recipient testes. Only EGFP-positive cells were gated for analysis. Red line, specific antibody; black line, isotype control.

(I) Serial transplantation. Appearance of abnormal colonies (left) and histological sections (right) of recipient testes. Both H-RasV12-GSCs (top) and cyD2E-GSCs (bottom) produced abnormal colonies. Extensive colonization of donor cells was observed (inset).

(J) CD44 expression in the secondary recipient testes.

Scale bar, 200 μm (A, C, and I); 100 μm (F and G). Error bars indicate SEM.

both types of recipients (4×10^6 cells) were transplanted into six different testes. Three months after transplantation, all testes showed colonization by both types of donor cells, and similar GCTs were observed (Figure 5I). The secondary recipients of H-RasV12-GSCs and cyD2E-GSCs showed abnormal spermatogenesis in 56.0% ± 3.6% (393/730 tubules in the six testes) and 53.5% ± 4.3% (282/544 tubules in the six testes) of the tubules, respectively. CD44 expression was evident by flow cytometry (Figure 5J).

DISCUSSION

Although a previous study showed that Ras is activated by GDNF in a SV40-transformed spermatogonia cell line (He et al.,

2008), the role of Ras in SSCs has not been assessed using functional criteria. We used a SSC transplantation assay to show that the activation of H-Ras is sufficient to induce SSC self-renewal. We also found that Ras isoforms have different biological properties on GSCs, despite the first 85 amino acids of all Ras isoforms being identical and their encompassing the site of interaction with all known Ras effectors (Malumbres and Barbacid, 2002). Ras isoforms seem to act differently in cells because of their cellular localizations (Omerovic et al., 2007). In fact, H-Ras can substitute for K-Ras during embryogenesis (Potenza et al., 2005). Likewise, the different properties of Ras isoforms in GSCs may also be explained by the differences in their cellular localization, rather than their catalytic activities. However, it should be noted here that Ras activation did not exclusively

Table 1. SSC Expansion in H-RasV12-and cyD2E-GSCs

Cell Type	Days to Transplant (Passage)[a]	Colonies/Testis	Colonies/10⁵ GSCs	Increase in Cell Number[b] (Fold)	Increase in Stem Cell Number[b] (Fold)
H-RasV12	14 (2)	17.0 ± 5.0	212.5 ± 62.5		
	43 (6)	9.5 ± 2.4	118.8 ± 30.1	266.9	149.2
	76 (11)	7.8 ± 1.5	96.9 ± 18.7	1.2×10^6	5.5×10^5
cyD2E	18 (3)	11.4 ± 2.2	142.5 ± 27.8		
	51 (8)	21.5 ± 4.4	268.8 ± 54.6	1321	2491
	78 (12)	19.3 ± 5.4	240.6 ± 67.6	1.3×10^6	2.2×10^6

Values are mean ± SEM. In each experiment, 8×10^3 cells were microinjected into the seminiferous tubules of infertile recipient testis.
[a] The number of days from initiation of culture to transplantation.
[b] The increase in the total cell or stem cell number from the initial transplantation.
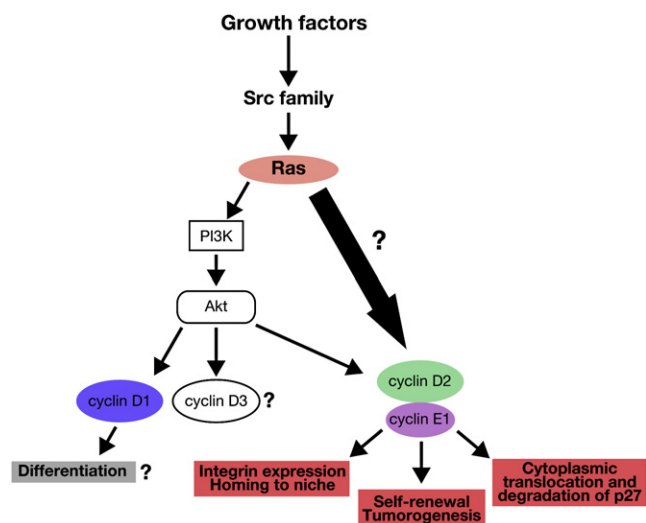
induce self-renewal division: we expected an increase in SSCs in transfected cells, but SSCs were not enriched in the culture, indicating that H-RasV12 did not change the proportion of self-renewal division. Moreover, H-RasV12-GSCs also underwent spermatogenesis in vivo and produced differentiating cells; Ras therefore seems to act before the decision is made to self-renew or to differentiate.

Among the numerous Ras effectors, the PI3K-Akt pathway is apparently involved in SSC self-renewal because inhibition of this pathway stops the proliferation of GSCs. However, the activation of Akt alone is not sufficient to drive SSC proliferation; Akt-GSCs require bFGF supplementation (Lee et al., 2007). Based on our results, we speculate that Ras activation also provided additional signals that are equivalent to bFGF signaling. This would explain why H-RasN17 interferes with GSC proliferation. Because Akt is only one of several downstream Ras effectors, inhibition of Akt-GSC proliferation by H-RasN17 suggests that H-RasN17 interferes with bFGF signaling. The molecule that cooperates with Akt remains to be identified, but it does not seem to belong to the MEK pathway, because adding MEK inhibitors had no effect on WT GSC growth. Although numerous Ras effectors exist, using GSC cultures is useful for delimiting the key components of SSC self-renewal, e.g., by complementing the growth of Akt-GSCs cultured in the absence of bFGF.

While these results demonstrate the involvement of Ras in SSC self-renewal, the next critical question was how SSCs distinguish among the different types of division in the nucleus. Although the loss of all D cyclins in irradiated animals abolishes the ability for long-term reconstitution of hematopoietic stem cells (Kozar et al., 2004), mice that lack all three D cyclins develop into the late gestation period (Kozar et al., 2004), and little is known about the function of cyclins in stem cells of other self-renewing tissues. We initially assumed that overexpression of cyclin D might mimic activated Ras, because overexpression of cyclin D can liberate cyclin E-cdk2 complexes from the inhibitory effects of p27 by transporting p27 into the cytoplasm. However, the same machinery may not operate in SSCs, in which p27 expression has not been detected (Beumer et al., 1999). Nevertheless, a recent study on mice deficient in Skp2, which mediates ubiquitin-dependent degradation of p27, showed progressive loss of spermatogenic cells (Fotovati et al., 2006), and the numbers of type A spermatogonia in p27-deficient mice are higher than those in the WT (Beumer et al., 1999). It was therefore still possible that p27 regulates SSC cell cycle. Although single

cyclin D transfection did not promote proliferation, cyclin E transfection induced efficient proliferation and colonization of SSCs when combined with cyclin D2.

The loss of SSC activity in cyD1E-GSCs and cyD3E-GSCs not only emphasizes the importance of using functional assays to study SSC but also suggests that cyclin expression is an important factor to SSC activity (Figure 6). The role of cyclin D2 in SSCs has been unclear. Despite its expression during the transition of undifferentiated spermatogonia into type A spermatogonia (Beumer et al., 2000), spermatogenesis can proceed without cyclin D2 (Sicinski et al., 1996). Although cyclin D shows only 50%–60% identity throughout the entire coding sequence, the functional redundancy of the cyclin family has complicated many cyclin studies. The differences among D-type cyclins appear to be limited mostly to their tissue-specific expression patterns (Sherr and Roberts, 2004). In fact, a knockin strain of mice that expresses cyclin D2 instead of cyclin D1 exhibits normal development of cyclin D1-dependent tissues (Carthon

Figure 6. A Model for SSC Self-Renewal
Growth signals are converted to Ras activation via Src family molecules. Ras transmits signals to activate the PI3K-Akt pathway as well as other unknown pathways that run parallel to it. Cyclins D2 and E coordinate to drive SSC self-renewing division by eliminating p27 from the nucleus and upregulating β1-integrin, whereas strong cyclin D1 expression may induce differentiation.

et al., 2005). Nevertheless, our study indicates that the specificity of G1 cyclin and its collaboration with G1/S cyclin are important for driving SSC self-renewal. Given the results of H-RasV12-GSCs, which could differentiate normally into sperm, cyclins may be more specialized in the decision between self-renewal and differentiating divisions by acting downstream of Ras. Perhaps, Ras may randomly push the cell cycle, and the type of division is dictated by cyclins. However, regulation of cyclin expression may not be simple; our results suggest a potential interaction among *cyclin* gene expression. For example, cyD3E-GSCs upregulated *cyclin D1* and *D2* despite relatively constant *cyclin D3* levels. Moreover, although the amounts of cyclin D2 and E in cyD1E-GSCs are close to those in cyD2E-GSCs, the former failed to make germ cell colonies after transplantation, suggesting that cyclin D1 induces differentiation of SSCs. However, although differentiation due to constitutive expression of cyclin D1 should counteract the self-renewing effects of cytokines, we did not observe impairment of GSC growth when the cells were cultured in the cytokines.

On the basis of these results, we speculate that the relative proportion, rather than the total amount, of cyclin D2 is important in SSC activity. Although the frequency of SSCs was not increased in the cyD2E-GSCs, increasing the cyclin D2 expression or decreasing the cyclin D1 expression may lead to more extensive colonization. How cyclins influence the fate of SSCs remains to be determined; however, limits of germ cell transplantation must also be kept in mind. It is estimated that ~90% of WT SSCs cannot reach niche (Nagano et al., 1999). By definition, the presence of SSCs cannot be detected unless they make visible germ cell colonies. In this context, the presence of a few cyD3E-GSCs in the tubules suggests that they might have reached the niche and retained self-renewal activity, because they would have died or differentiated by 3 months. Perhaps these cells are unable to differentiate due to abnormal cyclin expression. Alternatively, cyclin may influence the fate of SSCs by changing adhesion to niche via β1-integrin, which is an essential homing receptor for SSCs (Kanatsu-Shinohara et al., 2008a). The analysis of *cyclin* transfectants will lead us to the better understanding of SSC homing and subsequent colony development.

Another important observation from the transplantation experiment was the development of GCT. Activating mutations in *Ras* genes have been described at a frequency of ~10% in human GCTs (Goddard et al., 2007), and cyclin D2 overexpression is one of the earliest known aberrations in carcinoma in situ and in testicular GCT in humans (Bartkova et al., 2003; Looijenga et al., 2007). Ras-induced tumorigenesis is invasive probably because the activation of other Ras effectors may confer more aggressive phenotypes. A similar GCT model has been previously produced by the overexpression of GDNF in transgenic animals, in which all male mice also develop GCT that mimics classic seminomas (Meng et al., 2000, 2001). However, in that model, tumorigenesis took a considerable amount of time (~7 months–1 year), and the transgene was expressed ubiquitously in both somatic and germ cells, making it difficult to analyze the early stages and origin of tumorigenesis. Because only stem cells can seed and proliferate in the niche, our results imply that excessive activation of self-renewing machinery in SSCs trigger GCT. Thus cyclin appears to be involved in the delicate balance between tissue maintenance and tumorigenesis in the SSCs.

How did these self-renewing signals induce GCT? Ideally early steps of GCT development could be detected by morphological analysis. However, no apparent abnormalities were found in GSCs before transplantation. Or rather, normal spermatogenesis in H-RasV12-GSCs and the upregulation of CD44 strongly suggest that in vivo testicular microenvironment provided oncogenic signals that thus far have been missing in in vitro studies. Although we could not identify the signals involved, our method combining SSC transfection and germ cell transplantation provides an opportunity to detail the mechanism of GCT formation. It would also be interesting to examine whether SSCs from fetal and adult origins produce similar GCTs. In conclusion, we demonstrate that Ras activation and a specific combination of cyclins are critical for driving SSC self-renewal. In addition, excessive self-renewal signaling may induce GCT. Successful reconstruction of SSC self-renewal by genetic manipulation provides an important platform to further investigate self-renewal machinery and its relationship to cancer development.

EXPERIMENTAL PROCEDURES

Cell Culture and Transfection

WT and EGFP-expressing GSCs were cultured as previously described using Stempro34 (Kanatsu-Shinohara et al., 2003). Akt-Mer-GSCs have previously been described (Lee et al., 2007). We also produced Akt-GSCs by electroporating *pCAG-AktCA-IRES-Neo*, as described previously (Kanatsu-Shinohara et al., 2006). ESCs were cultured under standard conditions with leukemia inhibitory factor (Invitrogen, Carlsbad, CA). For virus transfection, cDNAs encoding human *H-RasV12* (gift from Dr. S. Yamanaka, Kyoto University) and human *H-RasN17* (Upstate Technology, Lake Placid, NY) were cloned into *CSII-EF-IRES2-hKO1* vector, whereas human *K-RasV12* (Addgene, Cambridge, MA), mouse *cyclin D1*, *D2*, or *D3*, or human *cyclin E1* (gifts from Dr. C.J. Sherr, Cold Spring Harbor Laboratory, New York, NY) were cloned into *CSII-EF-IRES2-Venus* vector. Both virus vectors expressed transgenes under *Eif1a* promoter (gift from Dr. H. Miyoshi, RIKEN BRC). Virus particles were produced by transient transfection of 293T packaging cells, as previously described (Kanatsu-Shinohara et al., 2008b). Cells were maintained on mitomycin C-treated MEFs. The infection efficiency (>99%) was monitored by hKO1 or Venus expression. All infection experiments were performed in 6-well plates using 3×10^5 GSCs.

The growth factors used were 20 ng/ml mouse EGF, 10 ng/ml human bFGF, and 15 ng/ml recombinant rat GDNF (all from Peprotech, London, UK). For inhibitor studies, PP2 (5 μM), LY294002 (33 μM), Akt inhibitor IV (40 nM), and PD98059 (25 μM) were added at the time of cell plating (all from Calbiochem, Tokyo, Japan). A laminin adhesion assay was performed by plating 2×10^5 cells in 12-well dishes coated with laminin (20 μg/ml; BD Biosciences, San Jose, CA). After 30 min, the adherent cells were recovered by trypsin, as previously described (Kanatsu-Shinohara et al., 2008a).

Flow Cytometry

The following primary antibodies were used: mouse anti-SSEA-1 (MC-480; Chemicon, Temecula, CA), rat anti-mouse EpCAM (G8.8), rat anti-human α6-integrin (CD49f) (GoH3), biotinylated hamster anti-rat β1-integrin (CD29) (Ha2/5), APC-conjugated rat anti-mouse c-kit (CD117) (2B8), rat IgG₁ (κ isotype control), and rat anti-mouse CD44 (KM114) (all from BD Biosciences). APC-conjugated goat anti-rat IgG (Cedarlane Laboratories, Burlington, ON, Canada), APC-conjugated streptavidin (BD Biosciences), and Alexa Fluor 633-conjugated goat anti-mouse IgM (Molecular Probes, Eugene, OR) were used as secondary antibodies. Stained cells were analyzed using the FACS-Calibur system (BD Biosciences), as described previously (Kanatsu-Shinohara et al., 2003). Cell-cycle analysis was performed by staining with Hoechst 33342 (Sigma, St. Louis, MO) at 12.5 μg/ml for 45 min at 37°C. Cells were analyzed on a FACSAria2 equipped with 375 nm UV laser (BD Biosciences).

Transplantation

Donor cells were microinjected into the seminiferous tubules of W mice via an efferent duct (Japan SLC, Shizuoka, Japan). Recipients were treated with anti-CD4 antibody (GK1.5) to induce tolerance to the donor cells (Kanatsu-Shinohara et al., 2003). For subcutaneous injections, $\sim2 \times 10^6$ cells were injected into KSN nude mice (Japan SLC). The Institutional Animal Care and Use Committee of Kyoto University approved all of the animal experimentation protocols.

Analysis of the Recipient Testes

Recipient testes were processed for paraffin sectioning after fixation and stained with hematoxylin and eosin. The number of tubule cross-sections showing (and not showing) spermatogenesis, defined as the presence of multiple layers of germ cells in the entire circumference of the seminiferous tubule, was counted for one section from each testis. SSC colonization levels were also evaluated by counting the number of germ cell colonies based on fluorescence under UV light. Colonies were defined as germ cell clusters longer than 0.1 mm occupying the entire circumference of the tubule.

Analysis of Gene Expression

Total RNA was isolated using Trizol reagent (Invitrogen). First-strand cDNA was synthesized using Superscript II (RNase H⁻ reverse transcriptase, Invitrogen) for RT-PCR. For quantifying mRNA expression using real-time PCR, StepOnePlus Real-Time PCR system and *Power* SYBR Green PCR Master Mix were used (Applied Biosystems, Warrington, UK). All transcript levels were normalized to those of *Hprt1*. The PCR conditions were 95°C for 10 min, followed by 40 cycles at 95°C for 15 s, and 60°C for 1 min. The experiments were performed on two independent samples. Each PCR was run in triplicate. The primers used for PCR are listed in Table S1.

COBRA

Genomic DNA was treated with sodium bisulfite, which deaminates unmethylated cytosines to uracils but does not affect 5-methylated cytosines. Amplified PCR products by specific primer sets were digested with the indicated restriction enzymes, which had recognition sequences containing CpG in the original unconverted DNA. PCR primers used in the experiments are listed in Table S1.

Western Blot Analysis

We used SDS-PAGE to separate cell lysates (20 μg), which were then transferred to Hybond-P membranes (Amersham Biosciences, Buckinghamshire, UK). For Ras activation assays, the cells were separated after incubation in a GST-Raf1-RBD column (Active Ras pull-down and detection kit; Thermo Scientific, Rockford, IL). The following primary antibodies were used: polyclonal rabbit anti-mouse Akt, polyclonal rabbit anti-mouse Akt-P (Ser 473), polyclonal rabbit anti-mouse p27, polyclonal rabbit anti-human cdk2, polyclonal rabbit anti-human cdk2-P (Thr 160), polyclonal rabbit anti-human Erk1/2-P, polyclonal rabbit anti-human cyclin D2 (Cell Signaling, Danvers, MA), mouse anti-human p27-P (Thr 187) (Invitrogen), and mouse anti-Ras (Thermo Scientific). Peroxidase-conjugated polyclonal anti-rabbit IgG and anti-mouse IgG were used as the secondary antibodies (Cell Signaling).

Immunohistochemistry

For staining histological sections, immunohistochemical staining was performed on paraffin-embedded sections using polyclonal rabbit antibodies against human PLAP (Santa Cruz Biotechnology, Santa Cruz, CA) using the avidin-biotin complex method. The color was developed in diaminobenzidine solution.

For staining of cultured cells, the cells were concentrated on glass slides, and fixed in 4% paraformaldehyde at 4°C for 15 min. The cells were stained using polyclonal rabbit anti-mouse p27 and polyclonal rabbit anti-human cyclin D2 (Cell Signaling), and Alexa Fluor 568-conjugated goat anti-rabbit IgG (Molecular Probes) was used to detect the primary antibodies.

Statistical Analysis

Results were presented as mean ± SEM. Data were analyzed by Student's t test.

REFERENCES

Bartkova, J., Rajpert-De, M., Skakkebaek, N.E., Lukas, J., and Bartek, J. (2003). Deregulation of the G1/S-phase control in human testicular germ cell tumors. APMIS *111*, 252–266.

Beumer, T.L., Kiyokawa, H., Roepers-Gajadien, H.L., van den Bos, L.A.C., Lock, T.M.T.W., Gademan, I.S., Rutgers, D.H., Koff, A., and de Rooij, D.G. (1999). Regulatory role of p27kip1 in the mouse and human testis. Endocrinology *140*, 1834–1840.

Beumer, T.L., Roepers-Gajadien, H.L., Gademan, I.S., Kal, H.B., and de Rooij, D.G. (2000). Involvement of the D-type cyclins in germ cell proliferation and differentiation in the mouse. Biol. Reprod. *63*, 1893–1898.

Braydish-Stolle, L., Kostereva, N., Dym, M., and Hofmann, M.-C. (2007). Role of Src family kinases and N-Myc in spermatogonial stem cell proliferation. Dev. Biol. *304*, 34–45.

Brinster, R.L., and Zimmermann, J.W. (1994). Spermatogenesis following male germ-cell transplantation. Proc. Natl. Acad. Sci. USA *91*, 11298–11302.

Carthon, B.C., Neumann, C.A., Das, M., Pawlyk, B., Li, T., Geng, Y., and Sicinski, P. (2005). Genetic replacement of cyclin D1 function in mouse development by cyclin D2. Mol. Cell. Biol. *25*, 1081–1088.

Danielsen, A.J., and Maihle, N.J. (2002). The EGF/ErbB receptor family and apoptosis. Growth Factors *20*, 1–15.

de Rooij, D.G., and Russell, L.D. (2000). All you wanted to know about spermatogonia but were afraid to ask. J. Androl. *21*, 776–798.

Fotovati, A., Nakayama, K., and Nakayama, K.I. (2006). Impaired germ cell development due to compromised cell cycle progression in Skp2-deficient mice. Cell Div. *1*, 4.

Goddard, N.C., McIntyre, A., Summersgill, B., Gilbert, D., Kitazawa, S., and Shipley, J. (2007). KIT and RAS signaling pathways in testicular germ cell tumors: new data and a review of the literature. Int. J. Androl. *30*, 337–349.

He, Z., Jiang, J., Kokkinaki, M., Golestaneh, N., Hofmann, M.C., and Dym, M. (2008). Gdnf upregulates c-Fos transcription via Ras/Erk1/2 pathway to promote mouse spermatogonial stem cell proliferation. Stem Cells *26*, 266–278.

Kanatsu-Shinohara, M., Ogonuki, N., Inoue, K., Miki, H., Ogura, A., Toyokuni, S., and Shinohara, T. (2003). Long-term proliferation in culture and germline transmission of mouse male germline stem cells. Biol. Reprod. *69*, 612–616.

Kanatsu-Shinohara, M., Ikawa, M., Takehashi, M., Ogonuki, N., Miki, H., Inoue, K., Kazuki, Y., Lee, J., Toyokuni, S., Oshimura, M., et al. (2006). Production of knockout mice by random and targeted mutagenesis in spermatogonial stem cells. Proc. Natl. Acad. Sci. USA *103*, 8018–8023.

Kanatsu-Shinohara, M., Takehashi, M., Takashima, S., Lee, J., Morimoto, H., Chuma, S., Raducanu, A., Nakatsuji, N., Fässler, R., and Shinohara, T. (2008a). Homing of mouse spermatogonial stem cells to germline niche depends on β1-integrin. Cell Stem Cell *3*, 533–542.

Kanatsu-Shinohara, M., Muneto, T., Lee, J., Takenaka, M., Chuma, S., Nakat-suji, N., Horiuchi, T., and Shinohara, T. (2008b). Long-term culture of male germline stem cells from hamster testes. Biol. Reprod. 78, 611–617.

Kozar, K., Ciemerych, M.A., Rebel, V.I., Shigematsu, H., Zagozdzon, A., Sicinska, E., Geng, Y., Yu, Q., Bhattacharya, S., Bronson, R.T., et al. (2004). Mouse development and cell proliferation in the absence of D-cyclins. Cell 118, 477–491.

Lee, J., Kanatsu-Shinohara, M., Inoue, K., Ogonuki, N., Miki, H., Toyokuni, S., Kimura, T., Nakano, T., Ogura, A., and Shinohara, T. (2007). Akt mediates self-renewal division of mouse spermatogonial stem cells. Development 134, 1853–1859.

Li, W., Zhu, T., and Guan, K.-L. (2004). Transformation potential of Ras isoforms correlate with activation of phosphatidylinositol 3-kinase but not ERK. J. Biol. Chem. 279, 37398–37406.

Looijenga, L.H., Gillis, A.J., Stoop, H.J., Hersmus, R., and Oosterhuis, J.W. (2007). Chromosomes and expression in human testicular germ-cell tumors: insight into their cell of origin and pathogenesis. Ann. N Y Acad. Sci. 1120, 187–214.

Malumbres, M., and Barbacid, M. (2002). Ras oncogenes: the first 30 years. Nat. Rev. Cancer 3, 7–13.

Meistrich, M.L., and van Beek, M.E.A.B. (1993). Spermatogonial stem cells. In Cell and Molecular Biology of the Testis, C. Desjardins and L.L. Ewing, eds. (New York: Oxford University Press), pp. 266–295.

Meng, X., Lindahl, M., Hyvönen, M.E., Parvinen, M., de Rooij, D.G., Hess, M.W., Raatikainen-Ahokas, A., Sainio, K., Rauvala, H., Lakso, M., et al. (2000). Regulation of cell fate decision of undifferentiated spermatogonia by GDNF. Science 287, 1489–1493.

Meng, X., de Rooij, D.G., Westerdahl, K., Saarma, M., and Sariola, H. (2001). Promotion of seminomatous tumors by targeted overexpression of glial cell line-derived neurotrophic factor in mouse testis. Cancer Res. 61, 3267–3271.

Nagano, M., Avarbock, M.R., and Brinster, R.L. (1999). Pattern and kinetics of mouse donor spermatogonial stem cell colonization in recipient testes. Biol. Reprod. 60, 1429–1436.

Oatley, J.M., and Brinster, R.L. (2008). Regulation of spermatogonial stem cell self-renewal in mammals. Annu. Rev. Cell Dev. Biol. 24, 263–286.

Omerovic, J., Laude, A., and Prior, I.A. (2007). Ras proteins: paradigms for compartmentalized and isoform specific signaling. Cell. Mol. Life Sci. 64, 2575–2589.

Potenza, N., Vecchione, C., Notte, A., De Rienzo, A., Rosica, A., Bauer, L., Affuso, A., De Felice, M., Russo, T., Poulet, R., et al. (2005). Replacement of K-Ras with H-Ras supports normal embryonic development despite inducing cardiovascular pathology in adult mice. EMBO Rep. 6, 432–437.

Sherr, C.J., and Roberts, J.M. (2004). Living with or without cyclins and cyclin-dependent kinases. Genes Dev. 18, 2699–2711.

Sicinski, P., Donaher, J.L., Geng, Y., Parker, S.B., Gardner, H., Park, M.Y., Robker, R.L., Richards, J.S., McGinnis, L.K., and Biggers, J.D. (1996). Cyclin D2 is an FSH-responsive gene involved in gonadal cell proliferation and oncogenesis. Nature 384, 470–474.

Slingerland, J., and Pagano, M. (2000). Regulation of the cdk inhibitor p27 and its deregulation in cancer. J. Cell. Physiol. 183, 10–17.

Susaki, E., Nakayama, K., and Nakayama, K.I. (2007). Cyclin D2 translocates p27 out of the nucleus and promotes its degradation at the G0-G1 transition. Mol. Cell. Biol. 27, 4626–4640.

Takahashi, M. (2001). The GDNF/RET signaling pathway and human diseases. Cytokine Growth Factor Rev. 12, 361–373.

Thisse, B., and Thisse, C. (2005). Functions and regulations of fibroblast growth factor signaling during embryonic development. Dev. Biol. 287, 390–402.

Visvader, J.E., and Lindeman, G.J. (2008). Cancer stem cells in solid tumors: accumulating evidence and unresolved questions. Nat. Rev. Cancer 8, 755–768.

Yan, J., Roy, S., Apolloni, A., Lane, A., and Hancock, J.F. (1998). Ras isoforms vary in their ability to activate raf-1 and phosphoinositide 3-kinase. J. Biol. Chem. 273, 24052–24056.